Optimal Transmission of Progressive Sources Based on the Error Probability Analysis of SM and OSTBC

Seok-Ho Chang, *Member, IEEE*, Pamela C. Cosman, *Fellow, IEEE*, and Laurence B. Milstein, *Fellow, IEEE*

Abstract—**This paper studies the optimal design of multimedia progressive communication systems that are combined with low-complex open-loop multiple-input multiple-output techniques. First, we analyze the behavior of the crossover point of the error probability curves for orthogonal space-time block codes (OSTBC) and spatial multiplexing (SM) with a zero-forcing linear receiver. We mathematically prove that, in the high signal-to-noise ratio (SNR) regime, for both the information outage probability and the uncoded bit error rate, as data rate increases, the crossover point for the error probability monotonically decreases, and the crossover point for the SNR monotonically increases. We prove that this holds, regardless of the numbers of transmit and receive antennas and the spatial multiplexing rate of OSTBC. We next show how those results can be exploited for the optimal transmission of progressive sources, such as embedded image, which require unequal target error rates in their bitstream. That is, the computational complexity involved with the optimal space-time coding of progressive bitstream can be decreased.**

Index Terms—**Bit error rate (BER), information outage probability, multimedia progressive sources, multiple-input multiple-output (MIMO) systems, orthogonal space-time block codes (OSTBC), spatial multiplexing (SM), zero-forcing linear receiver.**

I. Introduction

THE growing demand for multimedia services has invoked intense research on cross-layer design [1], which is particularly important for transmission over mobile radio channels. Multimedia progressive sources such as embedded image or scalable video [2]–[4], which are expected to have more prominence in the future, employ a mode of transmission such that as more bits are received, the source can be reconstructed with better quality at the receiver. However, these advances in source codecs have also rendered the encoded bitstreams very sensitive to channel impairments, which can be severe in mobile channels.

Multiple-input multiple-output (MIMO) channels are able to provide huge gains in terms of reliability and transmission rate. Spatial diversity schemes, such as orthogonal space-time block codes (OSTBC) [5], [6], can combat channel fading and increase link reliability. The OSTBC is an important subclass of linear STBC, in the sense that it has an extremely simple and optimal linear receiver, and it achieves the full diversity. Spatial multiplexing (SM) [7], [8] transmits independent data substreams on each transmit antenna and increases the transmission data rate. Since SM does not decouple the data substreams at the receiver, the complexity of the optimal maximum-likelihood decoding is quite high. As a result, it is of practical interest to look for suboptimal linear receivers.

In this paper, we study the optimal design of such a low-complex MIMO system for the transmission of multimedia progressive sources. We first compare OSTBC and SM from the viewpoint of their error probabilities. Note that the diversity–multiplexing tradeoff (DMT) [9] has become a standard tool in the characterization of the performance of space-time codes, in slowly varying fading channels at high signal-to-noise ratio (SNR) and the large spectral efficiency regime. On the other hand, our approach focuses on how the crossover point of the error probability curves for the space-time codes behaves in the high SNR regime. In some literature, the crossover point of the ergodic capacity curves is investigated: The work in [10] compares ergodic capacities of beamforming, double space-time transmit diversity, and SM with a zero-forcing (ZF) receiver, and shows that spatial correlation has an effect on the location of the crossover point. In a similar way, the work in [11] compares ergodic capacities of OSTBC and SM with a ZF receiver. On the other hand, we compare error probabilities, such as information outage probability and uncoded bit error rate (BER), of OSTBC and SM for arbitrary numbers of antennas. Note that some results for the uncoded BER with two transmit antennas were presented in [12] by the authors of this paper.

We mathematically prove the monotonic behavior of the crossover points as a function of the transmission data rate. That is, we show that as the data rate increases, the crossover point in error probability monotonically decreases, whereas that in the SNR monotonically increases; these results are strictly proven for arbitrary numbers of transmit and receive antennas, and the spatial multiplexing rate of OSTBC. Regarding the SM, our analysis is focused on a ZF linear receiver, in part since the joint probability distribution of the post-processing SNRs for that receiver is properly characterized such that error probability can be obtained in a closed form. Note that novel wireless communication systems are targeting very large spectral efficiencies because of hot spots and pico-cell arrangements [13]. For such systems employing high data rates, because of power

Manuscript received August 26, 2012; revised December 30, 2012; accepted January 5, 2013. Date of publication January 30, 2013; date of current version January 13, 2014. This research was supported by the National Science Foundation under grant number CCF-0915727, and by Basic Science Research Program through the National Research Foundation of Korea (NRF) funded by the Ministry of Education (2013R1A1A2065143). This paper was presented in part at the 2013 IEEE Military Communications Conference. The review of this paper was coordinated by Dr. N.-D. Dao.

S.-H. Chang was with Qualcomm Inc., San Diego, CA 92121-1714 USA. He is now with the Department of Mobile Systems Engineering, Dankook University, Yongin 448-701, Korea (e-mail: seokho@dankook.ac.kr).

P. C. Cosman and L. B. Milstein are with the Department of Electrical and Computer Engineering, University of California at San Diego, La Jolla, CA 92093-0407 USA (e-mail: pcosman@ucsd.edu; milstein@ece.ucsd.edu).

Color versions of one or more of the figures in this paper are available online at http://ieeexplore.ieee.org.

Digital Object Identifier 10.1109/TVT.2013.2243851

consumption, the use of low-complexity linear receivers may be mandatory.

Transmission of images or video over MIMO systems has been studied by some researchers. For example, in [14], the authors took advantage of spatial multiplexing to transmit scalable video streams, and the work in [15] studied progressive video transmission via spatial diversity schemes. Instead of those extreme designs (i.e., full spatial multiplexing or full spatial diversity), in [16]–[19], the tradeoff between spatial multiplexing and diversity was studied to minimize the distortion of the source. Specifically, in [17]–[19], the optimal point on the diversity–multiplexing tradeoff region for MIMO channels was investigated with information-theoretic approaches, based on the work in [9]. In [16], layered source coding in the MIMO system is considered. On the other hand, in this paper, we exploit our analysis of the crossover point for the optimal space-time coding of multimedia progressive sources. The progressive sources have the key feature that they have steadily decreasing importance for bits later in the stream, which makes unequal target error rates very useful. Our analysis for the crossover point is used to optimally assign OSTBC or SM techniques to each portion of the progressive bitstream to be transmitted over Rayleigh fading channels.

II. System Model

Consider a MIMO system with N_t transmit and N_r receive antennas communicating through a frequency flat-fading channel. A space-time codeword $\mathbf{S} = [\mathbf{s}_1\, \mathbf{s}_2 \cdots \mathbf{s}_T]$ of size $N_t \times T$ is transmitted over T symbol durations via N_t transmit antennas. At the kth time symbol duration, the transmitted and received signals are related by

$$\mathbf{y}_k = \mathbf{H}\mathbf{s}_k + \mathbf{n}_k, \quad k = 1, \ldots, T \tag{1}$$

where $\mathbf{y}_k$ is the $N_r \times 1$ received signal vector, $\mathbf{H}$ is the $N_r \times N_t$ channel matrix, and $\mathbf{n}_k$ is a $N_r \times 1$ zero-mean complex AWGN vector with $\mathcal{E}[\mathbf{n}_k \mathbf{n}_l^H] = \sigma_n^2 \mathbf{I}_{N_r} \delta(k-l)$, where $(\cdot)^H$ denotes Hermitian operation. We assume that the entries of $\mathbf{H}$ are independent identically distributed (i.i.d.) $\sim \mathcal{CN}(0,1)$ and that $\mathbf{H}$ is random but constant over the duration T of a codeword (quasi-static Rayleigh i.i.d. fading). Let γ_s denote SNR per symbol. We define $\gamma_s := \mathcal{E}[|(\mathbf{s}_k)_i|^2]/\sigma_n^2$, where $(\mathbf{s}_k)_i$ is the ith component of the transmit signal vector $\mathbf{s}_k$ $(i = 1, \ldots, N_t)$. Let N_s denote the number of symbols packed within a space-time codeword $\mathbf{S}$. The spatial multiplexing rate is defined as N_s/T. We assume no channel state information (CSI) at the transmitter and perfect CSI at the receiver.

III. Analysis for the Behavior of the Crossover Points of the Error Probability Curves

A. Average Uncoded BER

We first express the BER of the OSTBC for an M-ary square quadratic-amplitude modulation (QAM) constellation. A closed-form expression for the BER of such a constellation for single-input single-output (SISO) systems in an AWGN channel is given by [20, eq. (14)]. For OSTBC, the same constellation symbol, $(\mathbf{s}_k)_i$, is transmitted N_t times during T symbol durations; thus, for an M-ary QAM, the SNR per bit, γ_b, is given by $\gamma_b = N_t \times \gamma_s / \log_2 M$. The instantaneous post-processing SNR per symbol is given by $\gamma_s \|\mathbf{H}\|_F^2$, where $\|\cdot\|_F$ denotes the Frobenius norm. From these, it can be readily shown that the exact BER of the OSTBC for an M-ary square QAM is expressed as (2), shown at the bottom of the page, where

$$\mu(i) = \sqrt{\frac{3(2i+1)^2(\log_2 M)\gamma_b}{2N_t(M-1) + 3(2i+1)^2(\log_2 M)\gamma_b}}.$$

We next present the BER of the SM scheme. For a ZF receiver, the instantaneous post-processing SNR on each substream is known to be a chi-square random variable [21], [22]; thus, the exact BER expression is achievable. The SNR per bit is given by $\gamma_b = \gamma_s / \log_2 M$. The exact BER of SM with a ZF receiver for an M-ary square QAM, which is denoted by $P_{b,\mathrm{SM-ZF}}$, is given in [23, eq. (3.12)].

In the following, we will find the crossover point of the BER curves of OSTBC and SM with a ZF receiver. The BER expressions given by (2) and [23, eq. (3.12)] are polynomials in γ_b with degrees greater than four, even for the simplest case of a 2×2 channel matrix. For these equations, there exists no closed-form solution for the crossover point. Thus, we will explore the asymptotic regime of high SNR to analyze the peculiar behavior of the crossover point. For high SNR, the BER is dominated by the error function term having the minimum Euclidian distance. If we discard the terms having non-minimum Euclidian distances and use $\sqrt{x/(1+x)} \approx 1 - 1/(2x)$ for $x \gg 1$, we have

$$P_{b,\mathrm{OSTBC}} \approx P_{b,\mathrm{OSTBC}}^{\mathrm{app}} = \binom{2N_tN_r - 1}{N_tN_r} \times \frac{4(\sqrt{M}-1)}{\sqrt{M}\log_2 M} \left(\frac{N_t(M-1)}{6\log_2 M}\right)^{N_tN_r} \left(\frac{1}{\gamma_b}\right)^{N_tN_r}. \tag{3}$$

$$P_{b,\mathrm{OSTBC}} = \frac{4}{\sqrt{M}\log_2 M} \sum_{k=1}^{\log_2 \sqrt{M}} \sum_{i=0}^{(1-2^{-k})\sqrt{M}-1} \left[(-1)^{\left\lfloor \frac{i \cdot 2^{k-1}}{\sqrt{M}} \right\rfloor} \left(2^{k-1} - \left\lfloor \frac{i \cdot 2^{k-1}}{\sqrt{M}} + \frac{1}{2} \right\rfloor\right) \left(\frac{1-\mu(i)}{2}\right)^{N_tN_r} \times \sum_{j=0}^{N_tN_r-1} \left\{ \binom{N_tN_r - 1 + j}{j} \left(\frac{1+\mu(i)}{2}\right)^j \right\} \right] \tag{2}$$

In the same way, it can be shown that $P_{b,\mathrm{SM-ZF}}$ can be approximated as

$$P_{b,\mathrm{SM-ZF}} \approx P^{\mathrm{app}}_{b,\mathrm{SM-ZF}} = \binom{2(N_r-N_t)+1}{N_r-N_t+1} \times \frac{4(\sqrt{M}-1)}{\sqrt{M}\log_2 M}\left(\frac{M-1}{6\log_2 M}\right)^{N_r-N_t+1}\left(\frac{1}{\gamma_b}\right)^{N_r-N_t+1}. \quad (4)$$

We compare the BERs of OSTBC and SM under the condition that the transmission data rates of both are set to be equal. To do this, we employ m-ary QAM for the SM, and m^{N_t/r_s}-ary QAM for the OSTBC, where r_s denotes the spatial multiplexing rate of the OSTBC. Note that, for $N_t = 2$, the Alamouti scheme achieves rate $r_s = 1$, whereas $r_s = 3/4$ is the maximum achievable rate for $N_t = 3$ or 4 in the complex OSTBC [24]. We assume that $m \geq 4$ (i.e., QPSK) and $N_r \geq N_t \geq 2$. If we let $M = m^{N_t/r_s}$ in (3) and let $M = m$ in (4), we have

$$P^{\mathrm{app}}_{b,\mathrm{OSTBC}} = \binom{2N_tN_r-1}{N_tN_r}\frac{4r_s(m^{N_t/2r_s}-1)}{m^{N_t/2r_s}N_t\log_2 m} \times \left(\frac{r_s(m^{N_t/r_s}-1)}{6\log_2 M}\right)^{N_tN_r}\left(\frac{1}{\gamma_b}\right)^{N_tN_r}. \quad (5)$$

$$P^{\mathrm{app}}_{b,\mathrm{SM-ZF}} = \binom{2(N_r-N_t)+1}{N_r-N_t+1}\frac{4(\sqrt{m}-1)}{\sqrt{m}\log_2 m} \times \left(\frac{m-1}{6\log_2 m}\right)^{N_r-N_t+1}\left(\frac{1}{\gamma_b}\right)^{N_r-N_t+1}. \quad (6)$$

We find the SNR, γ_b^*, for which (5) and (6) are the same. It can be shown that γ_b^* is given by

$$\gamma_b^* = \left(\frac{\binom{2N_tN_r-1}{N_tN_r}r_s^{N_tN_r+1}\sqrt{m}}{\binom{2(N_r-N_t)+1}{N_r-N_t+1}6^{(N_r+1)(N_t-1)}N_t(\sqrt{m}-1)m^{N_t/2r_s}} \times \frac{(m^{N_t/2r_s}-1)(m^{N_t/r_s}-1)^{N_tN_r}}{(\log_2 m)^{(N_r+1)(N_t-1)}(m-1)^{N_r-N_t+1}}\right)^{\frac{1}{(N_r+1)(N_t-1)}}. \quad (7)$$

We will prove that γ_b^* is a strictly increasing function in m, under the condition that $m \geq 4$, $N_r \geq N_t \geq 2$, and $0 < r_s \leq 1$. We define function $f(m)$ as

$$f(m) = \frac{\sqrt{m}(m^{N_t/r_s}-1)}{(\sqrt{m}-1)(m-1)}\cdot\frac{m^{N_t/2r_s}-1}{m^{N_t/2r_s}} \times \left(\frac{m^{N_t/r_s}-1}{m-1}\right)^{N_tN_r-1}\left(\frac{m-1}{\log_2 m}\right)^{(N_r+1)(N_t-1)}. \quad (8)$$

Let $g(m) = \sqrt{m}(m^{N_t/r_s}-1)/((\sqrt{m}-1)(m-1))$ be the first factor of $f(m)$. Then, for $m \geq 4$, $N_t \geq 2$, and $0 < r_s \leq 1$, we have

$$\frac{dg(m)}{dm} = \left(\left(\frac{N_t}{r_s}-1\right)m^{N_t/r_s+1} - \left(\frac{N_t}{r_s}-\frac{1}{2}\right)m^{N_t/r_s}\sqrt{m} - \frac{N_t}{r_s}m^{N_t/r_s} + \left(\frac{N_t}{r_s}+\frac{1}{2}\right)\frac{m^{N_t/r_s}}{\sqrt{m}} + m - \frac{\sqrt{m}}{2} - \frac{1}{2\sqrt{m}}\right)\Big/\left((\sqrt{m}-1)(m-1)\right)^2 > 0 \quad (9)$$

where the inequality is derived from the following:

Let $h(m) = p(m)\cdot m^{N_t/r_s}/2\sqrt{m}$ be the first four terms of the numerator of $dg(m)/dm$, where

$$p(m) = 2\left(\frac{N_t}{r_s}-1\right)m\sqrt{m} - \left(\frac{2N_t}{r_s}-1\right)m - \frac{2N_t}{r_s}\sqrt{m} + \frac{2N_t}{r_s} + 1. \quad (10)$$

Then, $dp(m)/dm$ can be expressed as

$$\frac{dp(m)}{dm} = \frac{1}{\sqrt{m}}\left[\left(\left(\frac{N_t}{r_s}-1\right)\sqrt{m} - \frac{N_t}{r_s}\right) \times (3\sqrt{m}+1) + 2\sqrt{m}\right]. \quad (11)$$

Since $m \geq 4$, $N_t \geq 2$, and $r_s \leq 1$, we have

$$\left(\frac{N_t}{r_s}-1\right)\sqrt{m} - \frac{N_t}{r_s} \geq \frac{N_t}{r_s} - 2 \geq 0. \quad (12)$$

From (11) and (12), it follows that $dp(m)/dm > 0$. We also have $p(4) = -11 + 6N_t/r_s > 0$. Hence, for $m \geq 4$, we have $p(m) > 0$, which yields $h(m) > 0$. In addition, let $q(m) = m - \sqrt{m}/2 - 1/2\sqrt{m}$ be the last three terms of the numerator of $dg(m)/dm$. Since $m \geq 4$, we have $dq(m)/dm = (m(4\sqrt{m}-1)+1)/4m\sqrt{m} > 0$. Further, $q(4) = 11/4 > 0$. Thus, $q(m) > 0$ for $m \geq 4$. We showed that $h(m) > 0$ and $q(m) > 0$; thus, (9) holds.

Through some more steps, it can be shown that $f(m)$ is a strictly increasing function in m, under the condition that $m \geq 4$, $N_r \geq N_t \geq 2$, and $0 < r_s \leq 1$. From (7) and (8), it is seen that as alphabet size, m, increases, γ_b^* strictly increases, regardless of the numbers of transmit and receive antennas, and the spatial multiplexing rate of the OSTBC. If we substitute γ_b^*, which is given by (7), into (5), the corresponding BER, P_b^*, is given by

$$P_b^* = \frac{4r_s^{N_tN_r+1}}{N_t}\binom{2N_tN_r-1}{N_tN_r} \times \left(\frac{N_t\binom{2(N_r-N_t)+1}{N_r-N_t+1}}{r_s^{N_tN_r+1}\binom{2N_tN_r-1}{N_tN_r}}\right)^{\frac{N_tN_r}{(N_r+1)(N_t-1)}} \times \left(\frac{(\sqrt{m}-1)m^{N_t/2r_s}}{\sqrt{m}(m^{N_t/2r_s}-1)}\right)^{\frac{N_tN_r}{(N_r+1)(N_t-1)}} \times \frac{m^{N_t/2r_s}-1}{m^{N_t/2r_s}\log_2 m}\left(\frac{m-1}{m^{N_t/r_s}-1}\right)^{\frac{N_tN_r(N_r-N_t+1)}{(N_r+1)(N_t-1)}}. \quad (13)$$

We will prove that P_b^* is a strictly decreasing function in m, under the condition that $m \geq 4$, $N_r \geq N_t \geq 2$, and $0 < r_s \leq 1$. We define function $r(m)$ as

$$r(m) = \frac{m^{N_t/2r_s}-1}{m^{N_t/2r_s}\log_2 m}\left(\frac{\sqrt{m}-1}{m^{N_t/2r_s}-1}\cdot\frac{m^{N_t/2r_s}}{\sqrt{m}(m^{N_t/2r_s}+1)} \times \frac{m-1}{m^{N_t/2r_s}-1}\right)^{\frac{N_tN_r}{(N_r+1)(N_t-1)}} \times \left(\frac{m-1}{m^{N_t/r_s}-1}\right)^{\frac{N_tN_r(N_r-N_t)}{(N_r+1)(N_t-1)}}. \quad (14)$$

Let $s(m) = (m^{N_t/2r_s} - 1)/(m^{N_t/2r_s} \log_2 m)$ be the first factor of $r(m)$. In the following, for $m \geq 4$, $N_t \geq 2$, and $0 < r_s \leq 1$, we will show that

$$\frac{ds(m)}{dm} = m^{N_t/2r_s-1}\left(\frac{-1}{\ln 2}m^{N_t/2r_s} + \frac{N_t}{2r_s}\log_2 m + \frac{1}{\ln 2}\right) \Big/ \left(m^{N_t/2r_s}\log_2 m\right)^2 < 0. \tag{15}$$

Let $u(m) = -m^{N_t/2r_s}/\ln 2 + (N_t/2r_s)\log_2 m + 1/\ln 2$ be the second factor of the numerator of $ds(m)/dm$. Then, we have

$$\frac{du(m)}{dm} = \frac{N_t}{(2r_s \ln 2)m}(-m^{N_t/2r_s} + 1) < 0 \tag{16}$$

where the inequality follows from $m \geq 4$, $N_t \geq 2$, and $r_s \leq 1$. For $m = 4$, we have

$$u(4) = \frac{1 - 4^{N_t/2r_s}}{\ln 2} + \frac{N_t}{r_s}. \tag{17}$$

It will be shown that $u(4) < 0$. Let $v(k) = (1 - 4^k)/\ln 2 + 2k$, where $k = N_t/2r_s \geq 1$. Then, $dv(k)/dk = 2(1 - 4^k) < 0$, and $v(1) = -3/\ln 2 + 2 < 0$. Thus, $v(k) < 0$ for $k \geq 1$, which indicates that $u(4) < 0$. From this and (16), it follows that $u(m) < 0$ for $m \geq 4$. Hence, (15) holds.

It can also be proven that $r(m)$ is a strictly decreasing function in m, under the condition that $m \geq 4$, $N_r \geq N_t \geq 2$, and $0 < r_s \leq 1$. From (13) and (14), we have the result that as alphabet size, m, increases, P_b^* strictly decreases, for an arbitrary number of transmit and receive antennas, and the spatial multiplexing rate of OSTBC. Further, from (5) and (6), it can be shown that

$$\begin{aligned} P_{b,\mathrm{OSTBC}}^{\mathrm{app}} &< P_{b,\mathrm{SM-ZF}}^{\mathrm{app}} \quad \text{for} \quad \gamma_b > \gamma_b^* \\ P_{b,\mathrm{OSTBC}}^{\mathrm{app}} &> P_{b,\mathrm{SM-ZF}}^{\mathrm{app}} \quad \text{for} \quad \gamma_b < \gamma_b^*. \end{aligned} \tag{18}$$

Let $P_{b,1}^*$ and $\gamma_{b,1}^*$ denote the crossover point when a modulation alphabet size $m = M_1$ is employed, and $P_{b,2}^*$ and $\gamma_{b,2}^*$ denote the crossover point when an alphabet size $m = M_2$ is used. Suppose that $M_1 < M_2$. Then, from the given results, we have

$$\gamma_{b,1}^* < \gamma_{b,2}^* \quad \text{and} \quad P_{b,1}^* > P_{b,2}^*. \tag{19}$$

B. Information Outage Probability

The information outage probability of the OSTBC is given by [25]

$$P_{\mathrm{out,OSTBC}} = P\left[r_s \log_2\left(1 + \frac{\gamma_s}{r_s}\|\mathbf{H}\|_F^2\right) < R\right] \tag{20}$$

where R is the transmission data rate (bits/s/Hz). Using the cumulative density function (CDF) of $\|\mathbf{H}\|_F^2$, a chi-square random variable with $2N_tN_r$ degrees of freedom, it can be shown that

$$P_{\mathrm{out,OSTBC}} = 1 - \exp\left(-\frac{r_s}{\gamma_s}(2^{R/r_s} - 1)\right) \times \sum_{k=1}^{N_tN_r} \frac{1}{(k-1)!}\left(\frac{r_s}{\gamma_s}(2^{R/r_s} - 1)\right)^{k-1}. \tag{21}$$

For the SM scheme, we consider pure spatial multiplexing [13], [26], where data are split into several substreams, i.e., one for each transmit antenna, and each substream undergoes independent temporal coding to avoid complex joint decoding of substreams at the receiver. A horizontally encoded V-BLAST is a popular example. For this scheme, an outage event occurs when any of the substreams is in outage (i.e., any of the subchannels cannot support the data rate assigned to it). Thus, the information outage probability is given by [13], [27]

$$P_{\mathrm{out,SM-ZF}} = P\left[\bigcup_{k=1}^{N_t}\left\{\log_2(1 + \gamma_s\eta_k) < \frac{R}{N_t}\right\}\right] \tag{22}$$

where η_k is a chi-square random variable with $2(N_r - N_t + 1)$ degrees of freedom $(k = 1, \ldots, N_t)$ [21], [22]. Based on the assumption that the η_k's are independent for a ZF receiver [28]–[30], and using the CDF of a chi-square random variable, it can be shown that

$$P_{\mathrm{out,SM-ZF}} = 1 - \left[\exp\left(-\frac{1}{\gamma_s}(2^{R/N_t} - 1)\right) \times \sum_{k=1}^{N_r-N_t+1} \frac{1}{(k-1)!}\left(\frac{1}{\gamma_s}(2^{R/N_t} - 1)\right)^{k-1}\right]^{N_t}. \tag{23}$$

Next, we will find the crossover point of the outage probability curves of OSTBC and SM with a ZF receiver. Since the expressions given by (21) and (23) are not analytically tractable to obtain a closed-form solution of the crossover point, we consider high SNR approximate expressions. Using the Taylor series expansion, (21) can be rewritten as (24), shown at the bottom of the next page. For high SNR, if we use only the dominant terms in the numerator and denominator, then

$$P_{\mathrm{out,OSTBC}} \approx P_{\mathrm{out,OSTBC}}^{\mathrm{app}} = \frac{1}{(N_tN_r)!}\left(\frac{r_s}{\gamma_s}(2^{R/r_s} - 1)\right)^{N_tN_r}. \tag{25}$$

For the SM scheme, the high SNR approximate expression is given by [28]

$$P_{\mathrm{out,SM-ZF}} \approx P_{\mathrm{out,SM-ZF}}^{\mathrm{app}} = \frac{N_t}{(N_r - N_t + 1)!}\left(\frac{1}{\gamma_s}(2^{R/N_t} - 1)\right)^{N_r-N_t+1}. \tag{26}$$

We find the SNR, γ_s^*, for which (25) and (26) are the same. It can be shown that γ_s^* is given by

$$\gamma_s^* = \left(\frac{(N_r - N_t + 1)!\, r_s^{N_tN_r}(2^{R/r_s} - 1)^{N_tN_r}}{(N_tN_r)!\, N_t(2^{R/N_t} - 1)^{N_r-N_t+1}}\right)^{\frac{1}{(N_r+1)(N_t-1)}}. \tag{27}$$

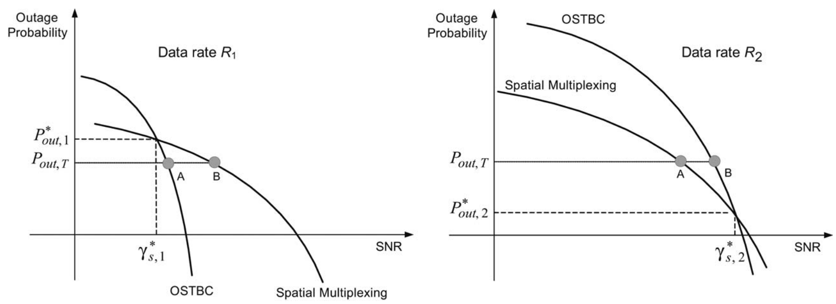

Fig. 1. High SNR approximate outage probabilities of OSTBC and SM with a ZF receiver for the given same transmission data rate. For data rate $R_1 < R_2$, these outage probabilities have the following properties: 1) $\gamma^*_{s,1} < \gamma^*_{s,2}$; 2) $P^*_{\text{out},1} > P^*_{\text{out},2}$; 3) $P^{\text{app}}_{\text{out},i,\text{OSTBC}} < P^{\text{app}}_{\text{out},i,\text{SM-ZF}}$ for $\gamma_{s,i} > \gamma^*_{s,i}$, and $P^{\text{app}}_{\text{out},i,\text{OSTBC}} > P^{\text{app}}_{\text{out},i,\text{SM-ZF}}$ for $\gamma_{s,i} < \gamma^*_{s,i}$ $(i = 1, 2)$. This figure can also be used to qualitatively depict the results, given by (18) and (19), for the uncoded BER.

We define the function $w(R)$ as

$$w(R) = \frac{(2^{R/r_s} - 1)^{N_t N_r}}{(2^{R/N_t} - 1)^{N_r - N_t + 1}} = \left(\frac{2^{R/r_s} - 1}{2^{R/N_t} - 1}\right)^{N_r - N_t + 1} (2^{R/r_s} - 1)^{(N_t - 1)(N_r + 1)}. \tag{28}$$

Let $y(R) = (2^{R/r_s} - 1)/(2^{R/N_t} - 1)$. Then, for $R > 0$, $N_t \geq 2$, and $0 < r_s \leq 1$, we have

$$\frac{dy(R)}{dR} = \frac{\ln 2}{r_s N_t} \cdot \frac{2^{R/r_s}\left((N_t - r_s)2^{R/N_t} - N_t\right) + r_s 2^{R/N_t}}{(2^{R/N_t} - 1)^2} > 0 \tag{29}$$

where the inequality is derived from the following: Let $z(R) = 2^{R/r_s}((N_t - r_s)2^{R/N_t} - N_t) + r_s 2^{R/N_t}$ be a factor of the numerator of $dy(R)/dR$. It is clear that $z(R)$ is monotonically increasing in R. Hence, for $R > 0$, we have $z(R) > z(0) = 0$, which indicates that (29) is valid.

From (27)–(29), it follows that γ^*_s is a strictly increasing function in R, under the condition that $R > 0$, $N_r \geq N_t \geq 2$, and $0 < r_s \leq 1$. If we substitute γ^*_s into (25), the corresponding outage probability, P^*_{out}, is given by

$$P^*_{\text{out}} = \frac{r_s^{N_t N_r}}{(N_t N_r)!}(2^{R/r_s} - 1)^{N_t N_r} \times \left(\frac{(N_t N_r)! N_t}{(N_r - N_t + 1)! r_s^{N_t N_r}} \cdot \frac{(2^{R/N_t} - 1)^{N_r - N_t + 1}}{(2^{R/r_s} - 1)^{N_t N_r}}\right)^{\frac{N_t N_r}{(N_r + 1)(N_t - 1)}}. \tag{30}$$

In a similar way, it can be proven that P^*_{out} is a strictly decreasing function in R, under the condition that $R > 0$, $N_r \geq N_t \geq 2$, and $0 < r_s \leq 1$. Hence, as the transmission data rate R increases, γ^*_s strictly increases, and P^*_{out} strictly decreases, regardless of the numbers of transmit and receive antennas, and the spatial multiplexing rate of OSTBC. Further, from (25) and (26), it can be shown that

$$\begin{aligned} P^{\text{app}}_{\text{out,OSTBC}} &< P^{\text{app}}_{\text{out,SM-ZF}} \quad \text{for} \quad \gamma_s > \gamma^*_s \\ P^{\text{app}}_{\text{out,OSTBC}} &> P^{\text{app}}_{\text{out,SM-ZF}} \quad \text{for} \quad \gamma_s < \gamma^*_s. \end{aligned} \tag{31}$$

Let $P^*_{\text{out},1}$ and $\gamma^*_{s,1}$ denote the crossover point when a transmission data rate $R = R_1$ is employed, and $P^*_{\text{out},2}$ and $\gamma^*_{s,2}$ denote the crossover point when a data rate $R = R_2$ is used. Suppose that $R_1 < R_2$. Then, from the results given, we have

$$\gamma^*_{s,1} < \gamma^*_{s,2} \quad \text{and} \quad P^*_{\text{out},1} > P^*_{\text{out},2}. \tag{32}$$

Based on (31) and (32), the high SNR approximate outage probabilities of OSTBC and SM with a ZF receiver for the given same data rate are qualitatively depicted in Fig. 1. Suppose that the target outage probability $P_{\text{out},T}$ is smaller than $P^*_{\text{out},1}$ but greater than $P^*_{\text{out},2}$. Then, from Fig. 1, it is seen that OSTBC is preferable to SM for a data rate R_1, whereas SM is preferable for a data rate R_2. Note that the results for the uncoded BER, given by (18) and (19), are coincidentally analogous to those for the information outage probability, which are given by (31) and (32). Hence, the same argument above can be made for the uncoded BER.

In [31], it is shown that outage probability and symbol error rate have a relationship at high SNR such that the two error probability curves differ only by a constant shift in SNR [31, Proposition 5], which indicates that the insight obtained from the outage probability can be applicable to the symbol error rate. However, the work in [31] considered the power outage probability given by [31, eq. (17)], which differs from the information outage probability considered in this paper. Note that information outage probability is closely related to the block error rate (BLER) of the system where a near-capacity

$$P_{\text{out,OSTBC}} = \frac{\sum_{k=1}^{\infty} \frac{1}{(k-1)!}\left(\frac{r_s}{\gamma_s}(2^{R/r_s} - 1)\right)^{k-1} - \sum_{k=1}^{N_t N_r} \frac{1}{(k-1)!}\left(\frac{r_s}{\gamma_s}(2^{R/r_s} - 1)\right)^{k-1}}{\sum_{k=1}^{\infty} \frac{1}{(k-1)!}\left(\frac{r_s}{\gamma_s}(2^{R/r_s} - 1)\right)^{k-1}} \tag{24}$$

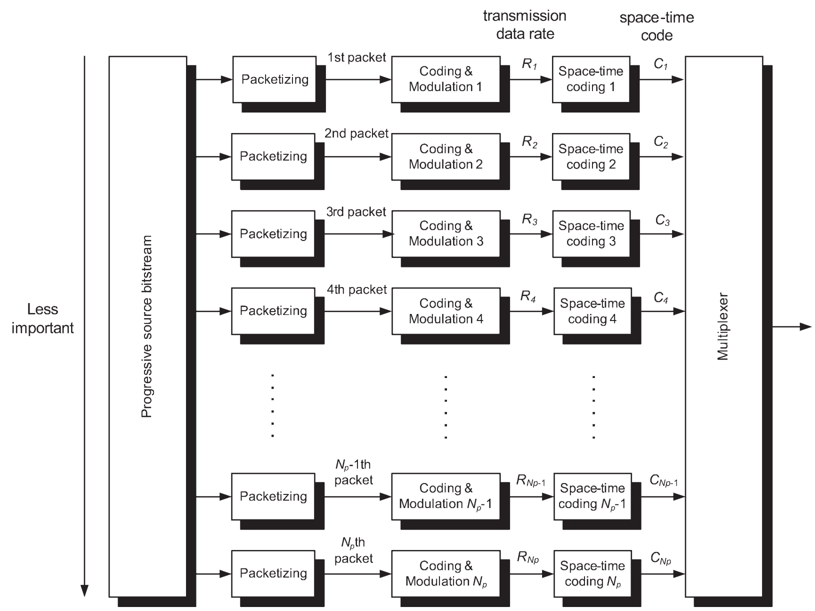

Fig. 2. Progressive source transmission system that is combined with open-loop MIMO techniques. R_i and C_i denote the transmission data rate and the space-time code assigned to the ith packet, respectively $(1 \leq i \leq N_P)$.

achieving code is employed. Further, the results in [31] apply to spatial diversity schemes but do not apply to SM schemes.

In Appendix A, we present discussion for the comparison between OSTBC and SM with an MMSE linear receiver.

IV. Optimal Space-Time Coding for the Transmission of Progressive Sources

The analysis in the previous section can be exploited to optimally design a low-complexity MIMO system for the transmission of the applications that require unequal target error rates or transmission data rates in their bitstream. In the following, we present the transmission of multimedia progressive sources [2]–[4].

Progressive encoders, which are promising technologies for multimedia communications, employ progressive transmission so that encoded data have gradual differences of importance in their bitstreams. Suppose that the system takes the bitstream from the progressive source encoder and transforms it into a sequence of N_P packets. Such a system is depicted in Fig. 2. Each of these N_P progressive packets can be encoded with different transmission data rates as well as different MIMO techniques when it is transmitted over mobile channels, so as to yield the best end-to-end performance as measured by the expected distortion of the source. The error probability of an earlier packet needs to be lower than or equal to that of a later packet, due to the gradually decreasing importance in the progressive bitstream. Thus, given the same transmission power, the earlier packet requires a transmission data rate that is lower than or equal to that of the later packet.

Let N_R denote the number of candidate transmission data rates employed by a system. The number of possible assignments of N_R data rates to N_P packets would exponentially grow as N_P increases. Further, in a MIMO system, if each packet can be encoded with different space-time codes (e.g., OSTBC or SM in this case), the assignment of space-time codes and data rates to N_P packets yields a more complicated optimization problem, compared with a SISO system. Note that each source, such as an image, has its inherent rate–distortion characteristic, from which the performance of the expected distortion is computed. Hence, for example, when a series of images is transmitted, the above optimization should be addressed in a real-time manner, considering which specific image (i.e., rate–distortion characteristic) is transmitted in the current time slot. To address this matter, for a SISO system, there have been some studies about the optimal assignment of data rates to a sequence of progressive packets [32]–[35].

For a MIMO system, we use the analytical results presented in the previous section to optimize the assignment of space-time codes to progressive packets. Recall that, for a progressive source, the error probability of an earlier packet needs to be lower than or equal to that of a later packet, and the earlier packet requires a transmission data rate that is lower than or equal to that of the later packet. Suppose that the kth packet in a sequence of N_P packets is encoded with SM. Then, our analysis tells us that the $k+1$st, $k+2$nd, $\ldots$, N_Pth packets should also be encoded with SM rather than with OSTBC. This is because we have proven that, when SM is preferable for a packet with a transmission data rate of R_1, a packet with a data rate of $R_2 (> R_1)$ should also be encoded with SM, as long as the target error rate of the latter is the same as or higher than that of the former (refer to Fig. 1). As a result, it can be shown that the number of possible assignments of space-time codes to N_P packets can be reduced by $2^{N_P}/(N_P+1)$ times, which indicates that the computational complexity involved with the optimization can be exponentially simplified. Note that a progressive bitstream is typically transformed into a sequence of numerous packets, in part because multiple levels of unequal error protection (UEP) are required for the progressive transmission. As an example, for the transmission of a 512 $\times$ 512 image with a rate of 1 bit per pixel (bpp), a sequence of 512 packets is considered in [32] (i.e., $N_P = 512$).

Lastly, we briefly describe the difference between the work in [16] and ours presented earlier. The authors of [16] considered layered source coding in the MIMO system; for the transmission of two unequally important source layers, the authors find the optimal assignment of the space-time codes with various multiplexing and diversity gains. That work differs from ours in that the former assumes the same modulation alphabet size for the space-time codes to be assigned. Accordingly, a space-time code with a higher diversity gain (but a lower multiplexing gain) provides a lower data rate and stronger error protection of the source. On the other hand, as described in [16], a space-time code with a higher multiplexing gain offers a higher data rate but retains weaker error protection ability. For this reason, in [16], the selection of space-time codes is necessarily related to the UEP of a layered source. From this, as shown in [16, Table I], it follows that a space-time code with a lower multiplexing gain should be used for the more important layer, whereas a space-time code with a higher multiplexing gain is used for the less important layer. On the other hand, in this paper, two space-time codes are compared under the condition that the transmission data rates of both are set to be equal (i.e., the modulation alphabet sizes are set to be different). Recall that the error probability of the more important layer needs to be lower than or equal to that of the less important layer, and given the same transmission power, the more important layer requires a transmission data rate that is lower than or equal to that of the less-important layer. In addition, recall that, in our analysis, two space-time codes are compared with the same transmission data rate, unlike the work in [16], which assumes the same modulation alphabet size for the space-time codes. From this, it follows that, without being related to a specific UEP strategy of a layered source, in this paper, a space-time code is selected for each layer (or each progressive packet), according to only the error probability performance; that is, a space-time code that exhibits a lower error probability for a given transmission data rate and a target error rate is selected (refer to Fig. 1).

V. Numerical Evaluation and Discussion

First, we numerically evaluate the outage probabilities and the uncoded BERs of OSTBC and SM with a ZF receiver for the same data rate. The error probabilities are evaluated in 2×4 MIMO systems for various data rates $R = 6$, 9, and 12 bits/s/Hz. The results are shown in Figs. 3 and 4, where solid curves denote the exact error probabilities, and dashed curves show the high SNR approximate error probabilities. The transmission data rate, R, and the size of QAM constellation, m, described below (4) are related by $R = N_t \log_2 m$ (bits/s/Hz). Figs. 3 and 4 show that, for both the outage probabilities and the BERs, the gap between the approximate crossover point and the exact one becomes smaller as transmission data rate increases.[1] For novel wireless communication systems targeting high data

[1]As indicated in Section III, this is because, as data rate increases, the crossover point in the SNR monotonically increases; hence, the high SNR approximate expressions become more accurate.

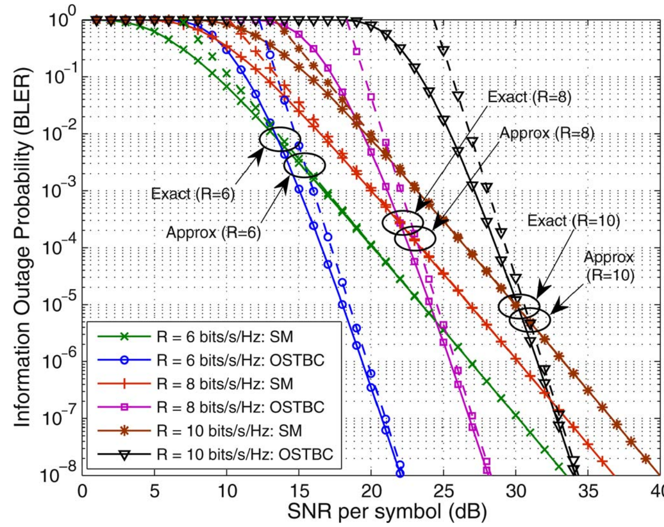

Fig. 3. Exact and high SNR approximate outage probabilities of OSTBC and SM with a ZF receiver for 2×4 MIMO systems in i.i.d. Rayleigh fading channels. Solid curves denote the exact outage probabilities, and dashed curves do the high SNR approximate outage probabilities. The exact and approximate crossover points are marked with circles.

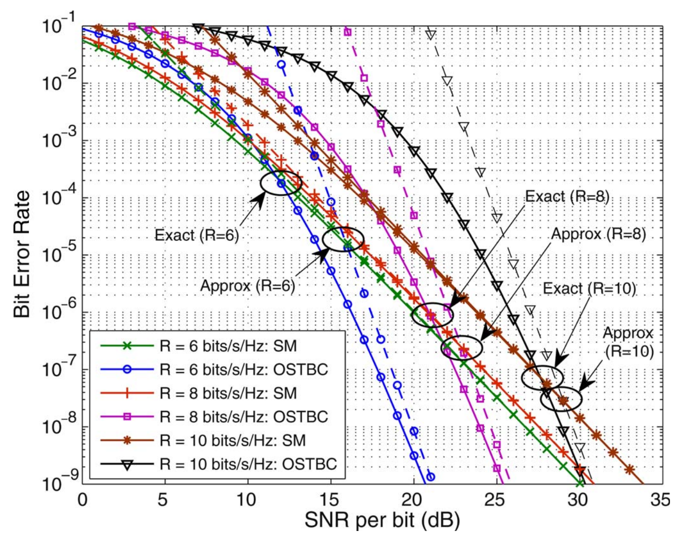

Fig. 4. Exact and high SNR approximate uncoded BERs of OSTBC and SM with a ZF receiver for 2×4 MIMO systems in i.i.d. Rayleigh fading channels. Solid curves denote the exact BERs, and dashed curves do the high SNR approximate BERs. The exact and approximate crossover points are marked with circles.

rates, the closed-form expressions of the approximate crossover points, given by (7), (13), (27), and (30), will become more accurate.

From Figs. 3 and 4, it is seen that as the data rate increases, the crossover point for the outage probabilities as well as the uncoded BERs behaves in a way predicted by the analysis given by (19) and (32) (refer to Fig. 1). If we focus on an outage probability of 10^{-3}, in Fig. 3, OSTBC outperforms SM for the data rate of 6 bits/s/Hz, whereas the latter outperforms the former for 8 bits/s/Hz. We note that this preference is a function of transmission data rate and the target outage probability of an application. For example, if the target is 10^{-1}, the SM outperforms the OSTBC even for the data rate of 6 bits/s/Hz.

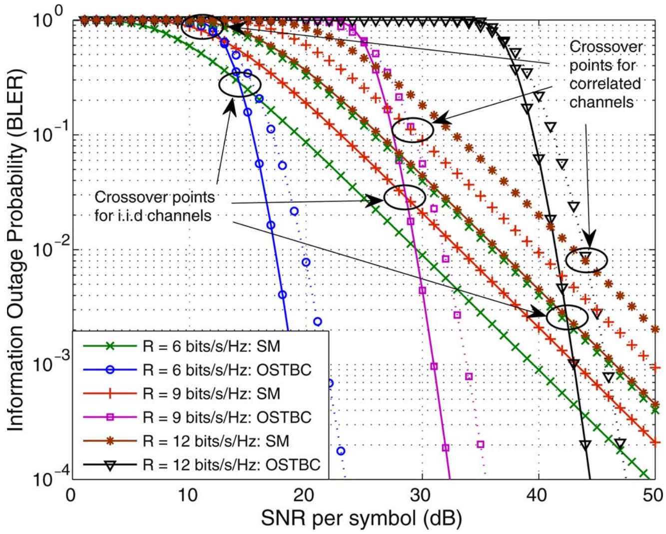

Fig. 5. Exact outage probabilities of OSTBC and SM with a ZF receiver for 3×3 MIMO systems in i.i.d. Rayleigh fading channels and spatially correlated Rayleigh fading channels with $\rho_t = \rho_r = 0.7$. Solid curves denote the exact outage probabilities for i.i.d. channels, and dotted curves do the exact outage probabilities for correlated channels. The crossover points are marked with circles.

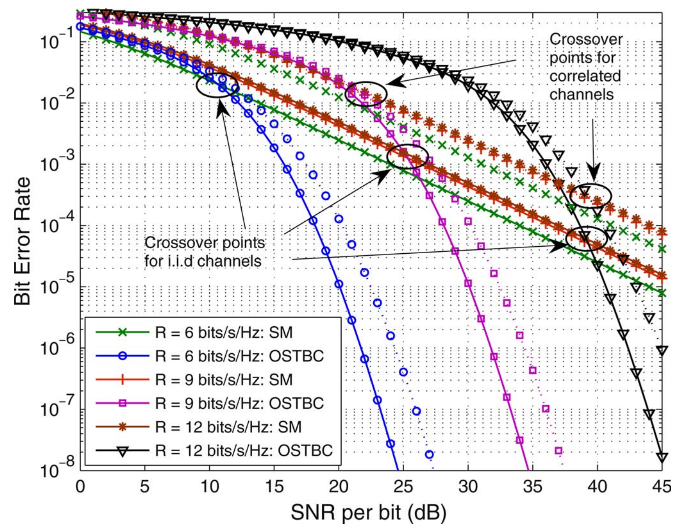

Fig. 6. Exact uncoded BERs of OSTBC and SM with a ZF receiver for 3×3 MIMO systems in i.i.d. Rayleigh fading channels and spatially correlated Rayleigh fading channels with $\rho_t = \rho_r = 0.7$. Solid curves denote the exact BERs for i.i.d. channels, and dotted curves do the exact BERs for correlated channels (the two BER curves for $R = 6$ bits/s/Hz in correlated channels merge at very low SNR, and is not depicted here). The crossover points are marked with circles.

A similar argument can be made for the uncoded BERs shown in Fig. 4.

In the following, instead of the i.i.d. MIMO Rayleigh fading channels described in Section II, we consider spatially correlated Rayleigh fading channels. Discussion for the analysis in the spatially correlated channels is presented in Appendix B. Here, we numerically investigate the behavior of the crossover point in those channels. MIMO channels with spatial correlation can be modeled as $\mathbf{H}_c = \mathbf{R}_r^{1/2}\mathbf{H}\mathbf{R}_t^{1/2}$ [36], where $\mathbf{R}_t$ is an $N_t \times N_t$ transmit spatial correlation matrix, $\mathbf{R}_r$ is an $N_r \times N_r$ receive spatial correlation matrix, $(\cdot)^{1/2}$ stands for the Hermitian square root of a matrix, and $\mathbf{H}$ is an $N_r \times N_t$ i.i.d. channel matrix as defined below (1). We use the exponential correlation model at the transmitter and the receiver with $(\mathbf{R}_t)_{i,j} = \rho_t^{|i-j|}$ and $(\mathbf{R}_r)_{i,j} = \rho_r^{|i-j|}$, where $(\cdot)_{i,j}$ denotes the (i, j)th element of a matrix, and ρ_t and ρ_r are the transmit and receive spatial correlation coefficients between adjacent antennas, respectively. The exact outage probabilities and BERs are evaluated, as an example, for 3×3 MIMO systems with various spatial correlation coefficients. The simulation results for $\rho_t = \rho_r = 0.7$ are shown in Figs. 5 and 6, where solid curves denote the error probabilities for i.i.d. channels, and dotted curves show the error probabilities for correlated channels. It is seen that the crossover points in the spatially correlated channels behave in the same way as do those for the i.i.d. Rayleigh fading channels.[2]

In Section IV, we presented the optimal space-time coding for the transmission of progressive sources. In the following, we will compare the performances of the optimal space-time coding and the suboptimal ones for progressive transmission. We evaluate the performances for 2×2 MIMO systems using the source coder SPIHT [37] as an example, and provide results for the standard 8 bpp 512×512 Lena image with a transmission rate of 0.5 bpp. We assume a slow fading channel such that channel coefficients are nearly constant over an image, and the channel estimation at the receiver is perfect. The end-to-end performance is measured by the expected distortion of the image.

In the following, we describe the evaluation of the expected distortion. The system takes a compressed progressive bitstream from the source encoder and transforms it into a sequence of packets with error detection and correction capability. Then, as shown in Fig. 2, the coded packets are encoded by the space-time codes. At the receiver, if a received packet is correctly decoded, the next packet is considered by the source decoder. Otherwise, the decoding is terminated, and the source is reconstructed from only the correctly decoded packets due to the nature of progressive source code.

Let $P_i(\dot{\gamma}_{s,i})$ denote the probability of a decoding error of the ith packet ($1 \le i \le N_P$), where $\dot{\gamma}_{s,i}$ is the instantaneous SNR per symbol for ith packet, and N_P is the number of packets. Then, the probability that no decoding errors occur in the first n packets with an error in the next one, $P_{c,n}$, is given by

$$P_{c,n}=P_{n+1}(\dot{\gamma}_{s,n+1})\prod_{i=1}^{n}(1-P_i(\dot{\gamma}_{s,i})), \quad 1\le n\le N_P-1. \tag{33}$$

Note that $P_{c,0} = P_1(\dot{\gamma}_{s,1})$ is the probability of an error in the first packet, and $P_{c,N_P} = \prod_{i=1}^{N_P}(1 - P_i(\dot{\gamma}_{s,i}))$ is the probability that all N_P packets are correctly decoded. Let $\{d_n\}$ denote the distortion of the source using the first n packets for the source decoder ($0 \le n \le N_P$). The $\{d_n\}$ can be expressed as $d_n = D(\sum_{i=1}^{n} r_i)$, where r_i is the number of source bits in ith packet, $D(x)$ denotes the operational distortion–rate function of the source, and $d_0 = D(0)$ refers to the distortion when the decoder reconstructs the source with none of the received information. Then, the expected distortion of the source, $E[D]$,

[2]For other spatial correlation coefficients, the corresponding crossover points also exhibit the same behavior; thus, they are not depicted here.

can be expressed as (34), shown at the bottom of the page, where $p(\dot{\gamma}_{s,i})$ is the probability density function (PDF) of the instantaneous SNR for ith packet, i.e., $\dot{\gamma}_{s,i}$. Note that $p(\dot{\gamma}_{s,i})$ is a function of the average SNR per symbol, γ_s, and the transmission data rate and the space-time code assigned to the ith packet; hence, $E[D]$ is also a function of those parameters. Let C_i denote the space-time code assigned to ith packet. One can find the optimal set of space-time codes $\mathbf{C}_{\text{opt}} = [C_1, \ldots, C_{N_P}]_{\text{opt}}$, which minimizes the expected distortion over a range of average SNRs using the weighted cost function as follows:

$$\arg\min_{C_1,\ldots,C_{N_P}} \frac{\int_0^\infty \omega(\gamma_s) E[D] d\gamma_s}{\int_0^\infty \omega(\gamma_s) d\gamma_s} \tag{35}$$

where $w(\gamma_s)$ in [0, 1] is the weight function. For example, $w(\gamma_s)$ can be given by

$$\omega(\gamma_s) = \begin{cases} 1, & \text{for } \gamma_s^A \le \gamma_s \le \gamma_s^B \\ 0, & \text{otherwise.} \end{cases} \tag{36}$$

Note that in broadcast or multicast systems, the weight function in (36) indicates that SNRs of multiple receivers are uniformly distributed in the range of $\gamma_s^A \le \gamma_s \le \gamma_s^B$. Equation (35) indicates that $C_1, \ldots, C_{N_P}$ are chosen such that the total sum of the expected distortion of the receivers distributed in the range of $\gamma_s^A \le \gamma_s \le \gamma_s^B$ is minimized. Note that the amount of computation involved in (35) exponentially grows as N_P increases. Alternatively, as presented in Section IV, we may choose the codes $C_1, \ldots, C_{N_P}$ with the constraint that the $k+1\text{st}, k+2\text{nd}, \ldots, N_P\text{th}$ packets should be encoded with SM (i.e., OSTBC is excluded) if the kth packet is encoded with SM.

To compare the image quality, we use the peak-signal-to-noise ratio (PSNR), defined as $10\log(255^2/E[D])$ (dB). We evaluate the PSNR performance as follows. We first compute (35) using the expected distortion, $E[D]$, given by (34), and the weight function, $w(\gamma_s)$, given by (36). Next, with the optimal set of codes, $\mathbf{C}_{\text{opt}} = [C_1, \ldots, C_{N_P}]_{\text{opt}}$, obtained from (35), we evaluate the PSNR over a range of SNRs given by (36). In this evaluation, error correction coding is not considered.

The performance is evaluated for the case when a sequence of 15 packets is transmitted (i.e., $N_P = 15$) as an example, and we assume that the transmission data rates are assigned in a manner such that $R_1 = R_2 = R_3 = 4$ (bits/s/Hz), $R_4 = R_5 = R_6 = 6$ (bits/s/Hz), $R_7 = R_8 = R_9 = 8$ (bits/s/Hz), $R_{10} = R_{11} = R_{12} = 10$ (bits/s/Hz), and $R_{13} = R_{14} = R_{15} = 12$ (bits/s/Hz), where R_i denotes the data rate employed by the ith packet. For this specific setup, the optimal set of space-time codes computed from (35) is given by $C_1 = C_2 = \cdots = C_6 = \text{OSTBC}$, and $C_7 = C_8 = \cdots = C_{15} = \text{SM}$. Fig. 7 shows the PSNR of such an optimal set of space-time codes, in addition to showing the PSNRs of other suboptimal sets of codes, such as the second best set of codes, the worst set of codes, and the sets at the 75th and 50th percentiles among the sets of codes (note that the number of possible sets of space-time codes is 2^{N_P}). Fig. 7 also shows the PSNR corresponding to the expected distortion that is averaged over all the possible sets of space-time codes. From this example, it is seen that PSNR performance of the progressive source tends to be sensitive to the way space-time codes are assigned to a sequence of packets, due to the unequal transmission data rates and target error rates of the progressive bitstream.

Fig. 8 shows the PSNR performance when (35) is computed with the constraint presented in Section IV (in this case, the number of possible sets of space-time codes is $N_P + 1$). For reference, some curves in Fig. 7 are repeated in Fig. 8. We note that the same optimal set of codes has been obtained when (35) is computed with and without the constraint. That is, without losing any PSNR performance, the computational complexity involved with the optimization can be reduced by exploiting the proof of the monotonic behavior of the crossover point, as shown in Fig. 1. It is also seen that the expected distortion averaged over all the possible sets of space-time codes becomes better when the constraint in Section IV is introduced, which shows that, on the average, the constraint in Section IV is a good strategy for the space-time coding of progressive sources.

VI. Conclusion

When progressive sources are transmitted over open-loop MIMO systems, due to the differences of importance in the bitstream, the tradeoff between the space-time codes should be clarified in terms of their target error rates and data rates. To address this matter, we analyzed the behavior of the crossover point of the error probability curves for OSTBC and SM with a ZF linear receiver. To make the analysis tractable, we explored the asymptotic regime of high SNR. Emerging wireless

$$\begin{aligned} E[D] &= \int_0^\infty \cdots \int_0^\infty \left\{ \sum_{n=0}^{N_P} (d_n P_{c,n}) \right\} p(\dot{\gamma}_{s,1}) \cdots p(\dot{\gamma}_{s,N}) d\dot{\gamma}_{s,1} \cdots d\dot{\gamma}_{s,N} \\ &= \int_0^\infty \cdots \int_0^\infty \left\{ D(0) P_1(\dot{\gamma}_{s,1}) + \sum_{n=1}^{N_P-1} \left(D\left(\sum_{i=1}^{n} r_i\right) P_{n+1}(\dot{\gamma}_{s,n+1}) \prod_{i=1}^{n} (1 - P_i(\dot{\gamma}_{s,i})) \right) \right. \\ &\quad \left. + D\left(\sum_{i=1}^{N_p} r_i\right) \prod_{i=1}^{N_P} (1 - P_i(\dot{\gamma}_{s,i})) \right\} p(\dot{\gamma}_{s,1}) \cdots p(\dot{\gamma}_{s,N}) d\dot{\gamma}_{s,1} \cdots d\dot{\gamma}_{s,N} \end{aligned} \tag{34}$$

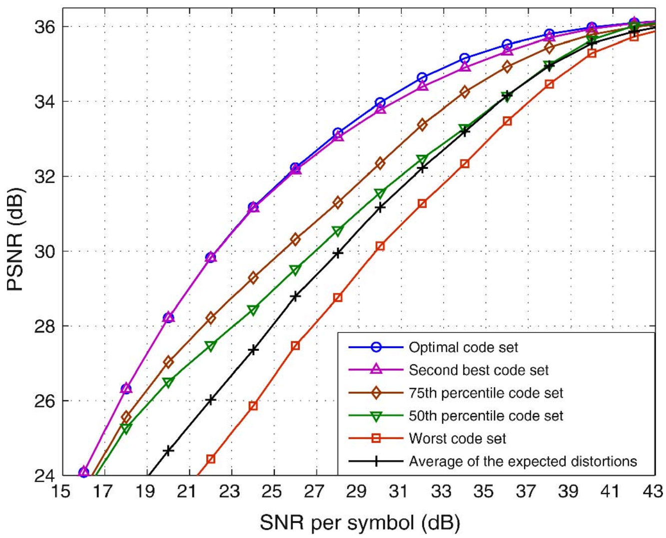

Fig. 7. PSNR performance of the optimal set of space-time codes and suboptimal ones for the transmission of progressive 8 bpp 512 × 512 Lena image for 2 × 2 MIMO systems in i.i.d. Rayleigh fading channels. 1) Optimal code set: $C_1 = \cdots = C_6 =$ OSTBC and $C_7 = \cdots = C_{15} =$ SM. 2) Second best code set: $C_1 = \cdots = C_6 =$ OSTBC, $C_7 = \cdots = C_{14} =$ SM, and $C_{15} =$ OSTBC. 3) 75th percentile code set: $C_1 =$ OSTBC, $C_2 = \cdots = C_{11} =$ SM, $C_{12} =$ OSTBC, $C_{13} = C_{14} =$ SM, and $C_{15} =$ OSTBC. 4) 50th percentile code set: $C_1 =$ OSTBC, $C_2 = C_3 = C_4 =$ SM, $C_5 =$ OSTBC, $C_6 =$ SM, $C_7 = \cdots = C_{11} =$ OSTBC, $C_{12} =$ SM, and $C_{13} = C_{14} = C_{15} =$ OSTBC. 5) Worst code set: $C_1 = C_2 =$ SM, $C_3 =$ OSTBC, $C_4 =$ SM, $C_5 =$ OSTBC, $C_6 =$ SM, $C_7 = \cdots = C_{11} =$ OSTBC, $C_{12} =$ SM, and $C_{13} = C_{14} = C_{15} =$ OSTBC.

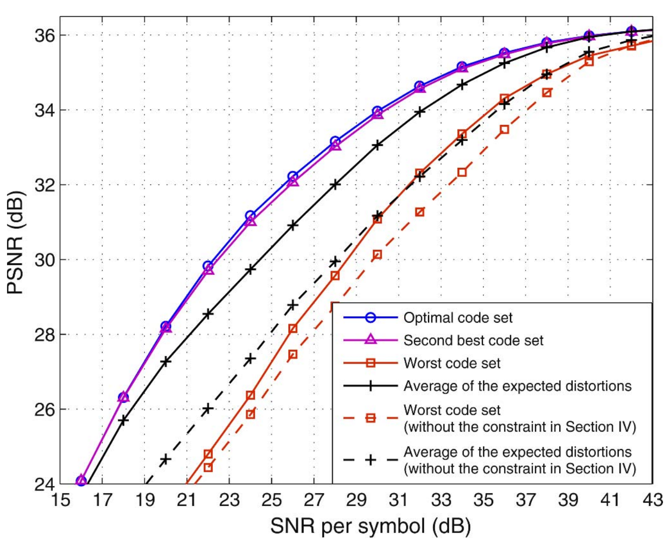

Fig. 8. PSNR performance of the optimal set of codes and suboptimal ones with the same setup as that in Fig. 7, except that (35) is computed with the constraint presented in Section IV. 1) Optimal code set: $C_1 = \cdots = C_6 =$ OSTBC and $C_7 = \cdots = C_{15} =$ SM. 2) Second best code set: $C_1 = \cdots = C_5 =$ OSTBC and $C_6 = \cdots = C_{15} =$ SM. 3) Worst code set: $C_1 = \cdots = C_{15} =$ SM.

communication systems are targeting large spectral efficiencies and will operate at high SNR, due to hot spots and pico-cell deployments. For such systems, the high SNR regime analysis will become more relevant. In addition, for a system with a large number of antennas and large spectral efficiencies, the use of low-complex space-time codes and linear receivers may be required, due to complexity and power consumption issues.

The analytical results for the information outage probability and the uncoded BER coincided such that, as data rate increases, the crossover point in error probability monotonically decreases, whereas that in the SNR monotonically increases. This was proven for an arbitrary number of transmit and receive antennas, and the spatial multiplexing rate of OSTBC (i.e., regardless of how the OSTBC is designed). As a result, for both the outage probability and the uncoded BER, our analysis allows a tradeoff between OSTBC and SM in terms of their target error rates and transmission data rates. These results, which are conceptually depicted in Fig. 1, to the best of our knowledge, have never been proven nor stated in a mathematical manner in the literature.

We next showed that those analytical results can be used to simplify the computations involved with the optimal space-time coding of a sequence of numerous progressive packets for the transmission of multimedia sources. The work in this paper has significance in terms of its impact on the area of multimedia communications and its analysis for the monotonic behavior of the crossover points, which deepens our understanding of the tradeoff between the space-time codes. This technical approach may be considered to analyze other codes such as quasi-OSTBC or the Golden code as future work.

Appendix A
Comparison Between OSTBC and SM With an MMSE Receiver

The outage probability for an MMSE receiver can be also expressed as (22). The marginal distribution of the post-processing SNR for an MMSE receiver is given by [38, eqs. (11)–(13)]. Since the N_t substream outage events are not independent for an MMSE receiver [28], the outage probability given by (22) cannot be computed with the marginal distribution. That is, we need the joint probability of the outage events, not just the marginal probabilities. To make the analysis tractable for an MMSE receiver, if we assume that the post-processing SNRs are statistically independent (this is the assumption used in [28]), the high SNR approximate outage probability can be expressed as [28, eq. (8)]. From this and (25), it can be shown that the crossover points in SNR and the outage probability are given by

$$\gamma_s^* = \left(\frac{(N_r - N_t + 1)! r_s^{N_t N_r} 2^{R(N_t-1)/N_t}}{(N_t N_r)!} \times \frac{(2^{R/r_s} - 1)^{N_t N_r}}{(2^{R/N_t} - 1)^{N_r}} \right)^{\frac{1}{(N_r+1)(N_t-1)}}. \tag{37}$$

$$P_{\text{out}}^* = \frac{r_s^{N_t N_r}}{(N_t N_r)!} \left(\frac{(2^{R/r_s} - 1)^{(N_r+1)(N_t-1)} (N_t N_r)!}{(N_r - N_t + 1)! r_s^{N_t N_r} 2^{R(N_t-1)/N_t}} \times \frac{(2^{R/N_t} - 1)^{N_r}}{(2^{R/r_s} - 1)^{N_t N_r}} \right)^{\frac{N_t N_r}{(N_r+1)(N_t-1)}}. \tag{38}$$

It can be proven that γ_s^* is a strictly increasing function of the data rate, R, under the condition that $N_r \geq N_t \geq 2$ and that $0 < r_s \leq 1$. On the other hand, it is not clear whether P_{out}^* is a strictly decreasing function of R under the same conditions, but we have been able to come up with a counterexample showing that P^*_{out} is not a strictly decreasing function for the case of $N_r = N_t = 2$ and $r_s = 1$ (i.e., the Alamouti coding). From this, it follows that the results for a ZF receiver do not always hold for an MMSE receiver. Further, we stress that the given outage probability analysis is based on the assumption that the post-processing SNRs are statistically independent for an MMSE receiver. Although some simulation results show that the assumption can be properly used [28], it is obvious that the given analysis is only approximately valid, even for high SNR. Regarding the BER analysis, the uncoded BER of an MMSE receiver can be expressed as $\int_0^\infty \sum_{i=1}^{\xi} \alpha_i Q(\sqrt{\beta_i x}) f(x) dx$, where $f(x)$ is the marginal PDF of the post-processing SNR given by [38, eqs. (11)–(13)], and α_i, β_i, and ξ are constants. Even for high SNR, it is not clear that the BER can be expressed in a closed form. For these reasons, we restricted the analysis of this paper to the case of a ZF linear receiver, for both the outage probability and the uncoded BER.

However, considering the fact that an MMSE receiver converges to a ZF receiver at high SNR, we do not exclude the possibility that, for a future work, there will be some mathematical analyses for an MMSE receiver which will produce the same results as those for a ZF receiver. In summary, since the joint distribution of the SNRs is not properly characterized, and the expectation of the Q-function with regard to the marginal distribution of the SNR is not analytically tractable, we restricted the scope of this paper to the case for a ZF linear receiver.

Appendix B
Comparison in the Spatially Correlated Rayleigh Fading Channels

For spatially correlated Rayleigh fading channels, the PDF of the post-processing SNR for OSTBC can be expressed as [39, eqs. (3) and (6)]. From this and [20, eq. (14)], the exact BER of M-ary QAM for OSTBC can be derived as [39, eqs. (6) and (8)–(10)]. For high SNR, we discard the Q-function terms having non-minimum Euclidean distances in [39, eq. (7)], and accordingly, only $i = 0$ is considered in [39, eq. (8)]. Further, if we use $\sqrt{x/(1+x)} \approx 1 - 1/(2x)$ for $x \gg 1$, [39, eq. (8)] can be approximated as

$$P_e^{M-PAM}(n;\rho) \approx \frac{1}{M\prod_{q=1}^{N}(c\rho\alpha_q)^{u_q}} B_{M,0} \sum_{q=1}^{N}\sum_{l=1}^{u_q} u_{q,l}(\rho) \times (c\rho\alpha_q)^l \left[\frac{1}{D_{M,0}^2 c\rho\alpha_q}\sum_{j=0}^{l-1}\binom{2j}{j}4^{-j}\left(1+\frac{D_{M,0}^2 c\rho\alpha_q}{2}\right)^{-j}\right] \tag{39}$$

where

$$\mu_{q,l}(\rho) = (-1)^{u_q - l}\sum_{\Phi}\prod_{j=1, j\neq q}^{N}\binom{u_j - 1 + i_j}{i_j} \times \left(\frac{1}{c\rho}\left(\frac{1}{\alpha_j} - \frac{1}{\alpha_q}\right)\right)^{-(u_j+i_j)}, \tag{40}$$

ρ is the SNR; $B_{M,0}$, $D_{M,0}$, and c are constants; and N, α_q, and u_q are parameters that are related to the eigenvalues of the Kronecker product of the transmit and receive spatial correlation matrices. In a similar way, we can derive a high SNR approximate BER for SM with a ZF receiver in spatially correlated channels. However, it is seen that, even for high SNR, the BER expression given by (39) and (40) is a complicated function of SNR, such that it is not clear whether there exists a closed-form solution for the crossover point of the BER curves for OSTBC and SM.

We now consider the information outage probability. For SM with a ZF receiver in spatially correlated channels, the marginal PDF of the post-processing SNR is characterized by [10, eq. (32)], and from this, the marginal CDF can be computed in a closed form [40]. Thus, the closed-form outage probability of a single substream can be readily derived. However, in spatially correlated channels, it is unclear whether N_t substream outage events are statistically independent. If they are not independent, we need the joint distribution of the post-processing SNRs for N_t substreams, which, to our knowledge, is not known. For these reasons, the analysis of this paper is restricted to the case of i.i.d. Rayleigh fading channels, for both the uncoded BER and the outage probability. However, in Section V, we present some numerical results for spatially correlated channels.

References

[1] Y. Shen, P. C. Cosman, and L. B. Milstein, "Video coding with fixed-length packetization for a tandem channel," *IEEE Trans. Image Process.*, vol. 15, no. 2, pp. 273–288, Feb. 2006.

[2] D. Taubman and M. Marcellin, *JPEG2000: Image Compression Fundamentals, Standards, and Practice*. Norwell, MA, USA: Kluwer, 2001.

[3] "Scalable Video Coding—Working Draft 1," in *Proc. Joint Video Team ITU-T VCEG ISO/IEC MPEG*, J. Reichel, H. Schwarz, and M. Wien, Eds., Hong Kong, Jan. 2005, CN, Doc. JVT-N020.

[4] H. Schwarz, D. Marpe, and T. Wiegand, "Overview of the scalable video coding extension of the H.264/AVC standard," *IEEE Trans. Circuits Syst. Video Technol.*, vol. 17, no. 9, pp. 1103–1120, Sep. 2007.

[5] S. M. Alamouti, "A simple transmit diversity technique for wireless communications," *IEEE J. Sel. Areas Commun.*, vol. 16, no. 8, pp. 1451–1458, Oct. 1998.

[6] V. Tarokh, H. Jafarkhani, and A. R. Calderbank, "Space-time block codes from orthogonal designs," *IEEE Trans. Inf. Theory*, vol. 45, no. 5, pp. 1456–1467, Jul. 1999.

[7] G. J. Foschini, "Layered space-time architecture for wireless communication in a fading environment when using multiple antennas," *Bell Labs. Tech. J.*, vol. 1, no. 2, pp. 41–59, Summer 1996.

[8] G. J. Foschini, G. D. Golden, R. A. Valenzuela, and P. W. Wolniansky, "Simplified processing for high spectral efficiency wireless communication employing multi-element arrays," *IEEE J. Sel. Areas Commun.*, vol. 17, no. 11, pp. 1841–1852, Nov. 1999.

[9] L. Zheng and D. N. C. Tse, "Diversity and multiplexing: A fundamental tradeoff in multiple-antenna channels," *IEEE Trans. Inf. Theory*, vol. 49, no. 5, pp. 1073–1096, May 2003.

[10] A. Forenza, M. R. McKay, A. Pandharipande, R. W. Heath, Jr., and I. B. Collings, "Adaptive MIMO transmission for exploiting the capacity of spatially correlated channels," *IEEE Trans. Veh. Technol.*, vol. 56, no. 2, pp. 619–630, Mar. 2007.

[11] A. Forenza, M. R. McKay, I. B. Collings, and R. W. Heath, Jr., "Switching between OSTBC and spatial multiplexing with linear receivers in spatially correlated MIMO channels," in *Proc. IEEE VTC*, Melbourne, Australia, May 2006, pp. 1387–1391.

[12] S.-H. Chang, M. Rim, P. C. Cosman, and L. B. Milstein, "Superposition MIMO coding for the broadcast of layered sources," *IEEE Trans. Commun.*, vol. 59, no. 12, pp. 3240–3248, Dec. 2011.

[13] K. Raj Kumar, G. Caire, and A. L. Moustakas, "Asymptotic performance of linear receivers in MIMO fading channels," *IEEE Trans. Inf. Theory*, vol. 55, no. 10, pp. 4398–4418, Oct. 2009.

[14] D. Song and C. W. Chen, "Scalable H.264/AVC video transmission over MIMO wireless systems with adaptive channel selection based on partial channel information," *IEEE Trans. Circuits Syst. Video Technol.*, vol. 17, no. 9, pp. 1218–1226, Sep. 2007.

[15] S. Zhao, Z. Xiong, X. Wang, and J. Hua, "Progressive video delivery over wideband wireless channels using space-time differentially coded OFDM systems," *IEEE Trans. Mobile Comput.*, vol. 5, no. 4, pp. 303–316, Apr. 2006.

[16] S. Lin, A. Stefanov, and Y. Wang, "On the performance of space-time block-coded MIMO video communications," *IEEE Trans. Veh. Technol.*, vol. 56, no. 3, pp. 1223–1229, May 2007.

[17] T. Holliday, A. J. Goldsmith, and H. V. Poor, "Joint source and channel coding for MIMO systems: Is it better to be robust or quick?" *IEEE Trans. Inf. Theory*, vol. 54, no. 4, pp. 1393–1405, Apr. 2008.

[18] R. Hormis, E. Linzer, and X. Wang, "Adaptive mode- and diversitycontrol for video transmission on MIMO wireless channels," *IEEE Trans. Signal Process.*, vol. 57, no. 9, pp. 3624–3637, Sep. 2009.

[19] H. Xiao, Q. Dai, X. Ji, and W. Zhu, "A novel JSCC framework with diversity–multiplexing-coding gain tradeoff for scalable video transmission over cooperative MIMO," *IEEE Trans. Circuits Syst. Video Technol.*, vol. 20, pp. 994–1006, Jul. 2010.

[20] K. Cho and D. Yoon, "On the general BER expression of one- and two-dimensional amplitude modulations," *IEEE Trans. Commun.*, vol. 50, no. 7, pp. 1074–1080, Jul. 2002.

[21] J. Winters, J. Salz, and R. D. Gitlin, "The impact of antenna diversity on the capacity of wireless communication systems," *IEEE Trans. Commun.*, vol. 42, no. 234, pp. 1740–1751, Feb.–Apr. 1994.

[22] D. Gore, R. W. Heath, Jr., and A. Paulraj, "On performance of the zero forcing receiver in presence of transmit correlation," in *Proc. IEEE Int. Symp. Info. Theory*, 2002, p. 159.

[23] S.-H. Chang, "Joint optimization of physical and application layers for wireless multimedia communications," Ph.D. dissertation, University of California, San Diego, CA, USA, 2010.

[24] X.-B. Liang, "Orthogonal designs with maximal rates," *IEEE Trans. Inf. Theory*, vol. 49, no. 10, pp. 2468–2503, Oct. 2009.

[25] C. Oestges and B. Clerckx, *MIMO Wireless Communications*. Orlando, FL, USA: Academic, 2007.

[26] A. Paulraj, R. Nabar, and D. Gore, *Introduction to Space-Time Wireless Communications*. Cambridge, U.K.: Cambridge Univ. Press, 2003.

[27] C. Papadias and G. Foschini, "On the capacity of certain space-time coding schemes," *EURASIP J. Appl. Signal Process.*, vol. 5, no. 1, pp. 447–458, May 2002.

[28] A. Hedayat and A. Nosratinia, "Outage and diversity of linear receivers in flat-fading MIMO channels," *IEEE Trans. Signal Process.*, vol. 55, no. 12, pp. 5868–5873, Dec. 2007.

[29] T. Guess, H. Zhang, and T. V. Kotchiev, "The outage capacity of BLAST for MIMO channels," in *Proc. IEEE ICC*, May 2003, pp. 2628–2632.

[30] N. Prasad and M. K. Varanasi, "Outage analysis and optimization for multiaccess and V-BLAST architecture over MIMO Rayleigh fading channels," in *Proc. 41st Annu. Allerton Conf. Commun., Control, Comput.*, Monticello, IL, USA, Oct. 2003, pp. 1–10.

[31] Z. Wang and G. B. Giannakis, "A simple and general parameterization quantifying performance in fading channels," *IEEE Trans. Commun.*, vol. 51, no. 8, pp. 1389–1398, Aug. 2003.

[32] V. Stankovic, R. Hamzaoui, Y. Charfi, and Z. Xiong, "Real-time unequal error protection algorithms for progressive image transmission," *IEEE J. Sel. Areas Commun.*, vol. 21, no. 10, pp. 1526–1535, Dec. 2003.

[33] A. Mohr, E. Riskin, and R. Ladner, "Unequal loss protection: Graceful degradation of image quality over packet erasure channels through forward error correction," *IEEE J. Sel. Areas Commun.*, vol. 18, no. 6, pp. 819–828, Jun. 2000.

[34] S.-S. Tan, M. Rim, P. C. Cosman, and L. B. Milstein, "Adaptive modulation for OFDM-based multiple description progressive image transmission," in *Proc. IEEE GLOBECOM*, New Orleans, LA, USA, Nov./Dec. 2008, pp. 1–5.

[35] D. G. Sachs, R. Anand, and K. Ramchandran, "Wireless image transmission using multiple-description based concatenated codes," in *Proc. SPIE*, San Jose, CA, USA, Jan. 2000, vol. 3974, pp. 300–311.

[36] E. G. Larsson and P. Stoica, *Space-time Block Coding for Wireless Communications*. Cambridge, U.K.: Cambridge Univ. Press, 2003.

[37] A. Said and W. A. Pearlman, "A new, fast, and efficient image codec based on set partitioning in hierarchical trees," *IEEE Trans. Circuits Syst. Video Technol.*, vol. 6, no. 3, pp. 243–250, Jun. 1996.

[38] H. Gao, P. J. Smith, and M. V. Clark, "Theoretical reliability of MMSE linear diversity combining in Rayleigh-fading additive interference channels," *IEEE Trans. Commun.*, vol. 46, no. 5, pp. 666–672, May 1998.

[39] I.-M. Kim, "Exact BER analysis of OSTBCs in spatially correlated MIMO channels," *IEEE Trans. Commun.*, vol. 54, no. 8, pp. 1365–1373, Aug. 2006.

[40] M. R. Spiegel, *Mathematical Handbook of Formulas and Tables*. New York, NY, USA: McGraw-Hill, 1991, ser. Schaum's Outline Series.

Seok-Ho Chang (S'07–M'10) received the B.S. and M.S. degrees in Electrical Engineering from Seoul National University, Seoul, Korea, in 1997 and 1999, respectively, and the Ph.D. degree in Electrical Engineering from the University of California, San Diego, CA, in 2010.

From 1999 to 2005, he was with LG Electronics, Korea, where he was involved in development of WCDMA (3GPP) base/mobile station modem chips. In 2006, he was with POSCO ICT, Korea, and worked on mobile WiMax systems. From 2010 to 2011, he was with the University of California, San Diego, CA as a Postdoctoral Scholar, where he was engaged in the cross layer design of wireless systems. From 2011 to 2012, he was with Qualcomm Inc., San Diego, CA as a Staff Engineer, where he was involved in design and development of 4G cellular modem chips. Since September 2012, he has been an Assistant Professor with the Department of Mobile Systems Engineering, Dankook University, Yongin, Korea. His research interests include wireless/wireline digital communication theory, signal processing, multi-user information theory, time and frequency synchronization, equalization, multiple-input multiple-output (MIMO) systems, and cross layer design of wireless systems.

Pamela C. Cosman (S'88–M'93–SM'00–F'08) obtained her B.S. degree with Honors in Electrical Engineering from the California Institute of Technology in 1987, and her M.S. and Ph.D. in Electrical Engineering from Stanford University in 1989 and 1993, respectively.

She was an NSF postdoctoral fellow at Stanford University and a Visiting Professor at the University of Minnesota during 1993–1995. In 1995, she joined the faculty of the department of Electrical and Computer Engineering at the University of California, San Diego, where she is currently a Professor. She was the Director of the Center for Wireless Communications from 2006 to 2008. Her research interests are in the areas of image and video compression and processing, and wireless communications.

Dr. Cosman is the recipient of the ECE Departmental Graduate Teaching Award, a Career Award from the National Science Foundation, a Powell Faculty Fellowship, and a Globecom 2008 Best Paper Award. She was a guest editor of the June 2000 special issue of the IEEE JOURNAL ON SELECTED AREAS IN COMMUNICATIONS on "Error-resilient image and video coding" and was the Technical Program Chair of the 1998 Information Theory Workshop in San Diego. She was an associate editor of the IEEE COMMUNICATIONS LETTERS (1998–2001), and an associate editor of the IEEE SIGNAL PROCESSING LETTERS (2001–2005). She was the Editor-in-Chief (2006–2009) as well as a Senior Editor (2003–2005, 2010–present) of the IEEE JOURNAL ON SELECTED AREAS IN COMMUNICATIONS. She is a member of Tau Beta Pi and Sigma Xi.

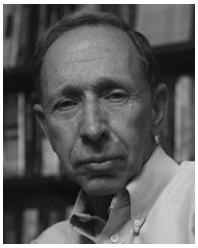

Laurence B. Milstein (S'66–M'68–SM'77–F'85) received the B.E.E. degree from the City College of New York, New York, NY, in 1964, and the M.S. and Ph.D. degrees in electrical engineering from the Polytechnic Institute of Brooklyn, Brooklyn, NY, in 1966 and 1968, respectively.

From 1968 to 1974, he was with the Space and Communications Group of Hughes Aircraft Company, and from 1974 to 1976, he was a member of the Department of Electrical and Systems Engineering, Rensselaer Polytechnic Institute, Troy, NY. Since 1976, he has been with the Department of Electrical and Computer Engineering, University of California at San Diego, La Jolla, where he is the Ericsson Professor of Wireless Communications Access Techniques and former Department Chairman, working in the area of digital communication theory with special emphasis on spread-spectrum communication systems. He has also been a consultant to both government and industry in the areas of radar and communications.

Dr. Milstein was an Associate Editor for Communication Theory for the IEEE TRANSACTIONS ON COMMUNICATIONS, an Associate Editor for Book Reviews for the IEEE TRANSACTIONS ON INFORMATION THEORY, an Associate Technical Editor for the *IEEE Communications Magazine*, and the Editor-in-Chief of the IEEE JOURNAL ON SELECTED AREAS IN COMMUNICATIONS. He was the Vice President for Technical Affairs in 1990 and 1991 of the IEEE Communications Society, and is a former Chair of the IEEE Fellows Selection Committee. He is a recipient of the 1998 Military Communications Conference Long Term Technical Achievement Award, an Academic Senate 1999 UCSD Distinguished Teaching Award, an IEEE Third Millennium Medal in 2000, the 2000 IEEE Communication Society Armstrong Technical Achievement Award, and various prize paper awards, including the 2002 MILCOM Fred Ellersick Award.